

TWO-STEP CASCADES FOLLOWING THERMAL NEUTRON CAPTURE IN
 ^{27}Al

JAROSLAV HONZÁTKO^a, VALERY A. KHITROV^b, ANATOLY M. SUKHOVOJ^b
and IVO TOMANDL^a

^a*Nuclear Physics Institute, CZ-25068 Řež near Prague, Czech Republic*

^b*Frank Laboratory of Neutron Physics, Joint Institute for Nuclear Research, 141980
Dubna, Russia*

Received 20 March 2003; revised manuscript received 11 December 2003

Accepted 15 December 2003 Online 19 April 2004

Cascades of two successive γ -transitions following thermal neutron capture in ^{27}Al have been studied. From $\gamma - \gamma$ coincidences accumulated in the experiment, 13 intensity distributions of two-step cascades terminating at low-lying levels of ^{28}Al have been determined. From these spectra, the energies of γ -transitions and intensities of 249 cascades populating 123 intermediate levels were derived. Energy dependence of intensity summed over the 0.5 MeV energy intervals for the cascades to two lower levels has also been determined.

PACS numbers: 25.40.LW, 27.30.+t

UDC 539.172.4

Keywords: thermal neutron capture in ^{27}Al , $\gamma - \gamma$ cascade coincidences, 123 intermediate levels of ^{28}Al , energy dependence of intensity

1. Introduction

Two-step cascades following thermal neutron capture were previously studied in experiments performed in Dubna, Riga and Řež for approximately 50 nuclei. Most investigated nuclei have large capture cross-sections for thermal neutrons. Therefore, the probabilities of background coincidences of two cascade quanta in the construction material of a spectrometer as compared to the real coincidences in the studied nucleus were negligible. The situation became complicated when we began to study the target nuclei with small thermal neutron capture cross-sections at the spectrometer in Řež.

The main source of background is the neutron capture in Al and Ge, in spite of the presence of effective shielding of the spectrometer from the scattered ther-

mal neutrons [1]. This background must be taken into account in data processing when the total energies of cascades in the studied nucleus and in the construction materials coincide within the energy resolution of the spectrometer. Therefore, a detailed study of the spectra of two-step cascades in the construction materials was undertaken, and that determined the choice of the nucleus studied in this work.

2. Experiment

The experiment was performed with the thermal neutron beam at the LWR-15 reactor in Řež. $\gamma - \gamma$ coincidences were registered with two HPGe detectors with 28% and 25% efficiency, respectively. The use of detectors with a higher efficiency does not change the conditions described in Ref. [1] of the experiment and estimation of possible systematical errors. Coincidence events were stored on a hard disk and were analysed with the standard method [2] based on the sum coincidence principle. The most informative part of this spectrum is shown in Fig. 1. Full energy peaks in this spectrum are labeled by the excitation energies of the final levels of the two-step cascades. Some peaks correspond to the escape of one to four annihilation quanta from the two detectors. Some peaks correspond to the registration of the first and third or two last quanta from the cascades with three or more quanta. As in the case of nuclei studied earlier, the measured spectra of cascades in ^{28}Al contain resolved peaks related with the most intense cascades, a

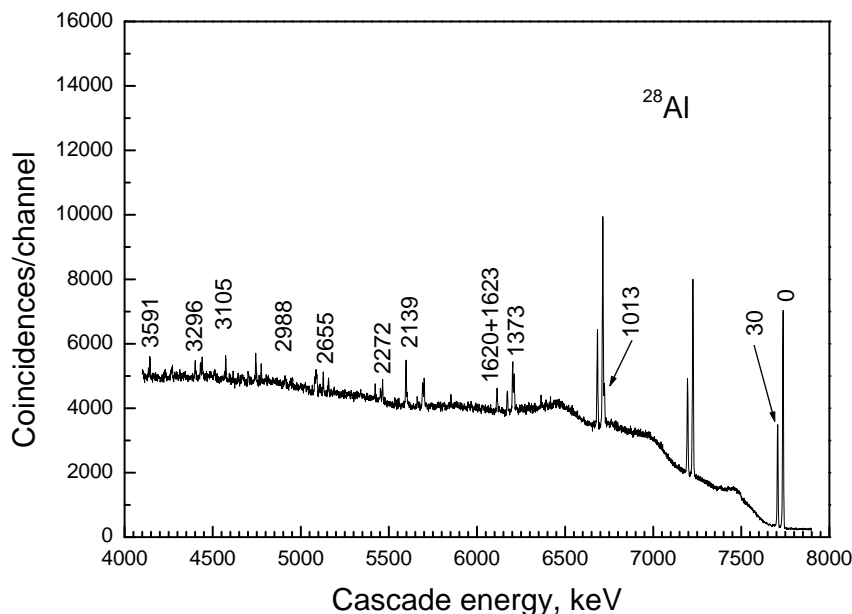


Fig. 1. Main part of the sum coincidence spectrum of ^{28}Al . Full-energy peaks are labelled with the energy (in keV) of the final cascade levels.

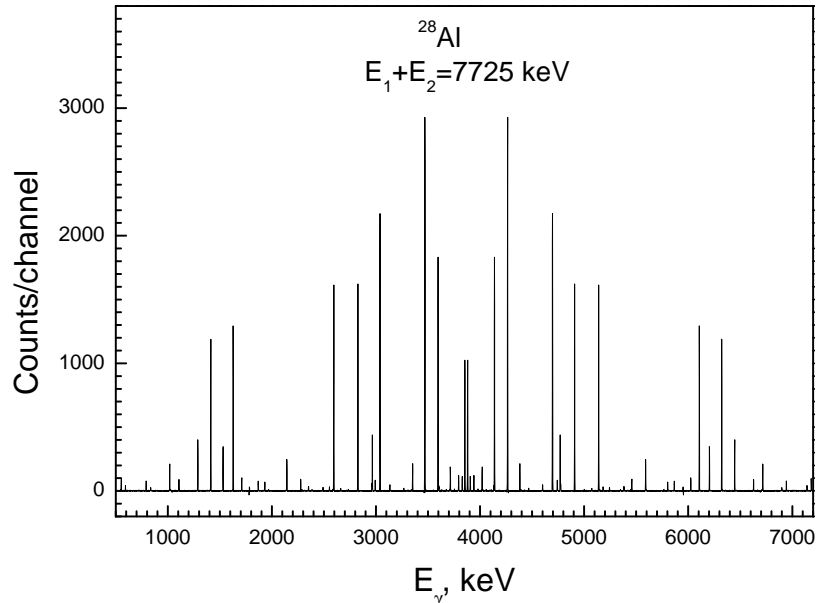


Fig. 2. Spectrum of the two-step γ -cascades terminating at the ground state of ^{28}Al .

pseudo-continuous distribution formed by a number of low-intensity cascades and a “noise” distribution with the zero mean value – the result of the background subtraction under a peak based on the sum coincidence spectrum. The use of the method of improvement of the resolution [3] allowed the construction of the spectra with the resolution varying from 1.8 keV at their ends to 3.0 keV in centre. As an example, Fig. 2 demonstrates intensity distribution of cascades to the ground-state of ^{28}Al . The differences and advantages of the sum-coincidence method as compared with the standard method are described in detail in Ref. [4]. Only the coincidence method allows one to get the information on the excited levels of any nucleus practically up the neutron binding energy. From 13 such spectra, transition energies and intensities of 249 cascades were obtained. Using the method of Ref. [5], a large part of them was unambiguously placed into the decay scheme up to the energy of $\approx B_n - 520$ keV. Cascades with the energies of their intermediate levels corresponding to the known ones are listed in Table 1, and other in Table 2. For the cascades with the energy of one or both transitions below 520 keV, only the lower estimate of intensity was obtained owing to the experimental conditions. The level energies in ^{28}Al were determined experimentally with a good precision, and the decay scheme of this nucleus needs a marked correction. About 34% of the cascade secondary transitions shown in Table 1 are now placed into the decay scheme for the first time.

The areas under the resolved peaks were transformed into the absolute intensities by the normalization to the absolute intensities i_1 [6] of some primary transitions, multiplied by branching ratios b of the corresponding secondary transi-

TABLE 1. A list of absolute intensities (per 10^5 decays), $i_{\gamma\gamma}$, of measured two-step cascades and energies, E_1 and E_2 , of the cascade transitions. E_i are energies of the intermediate levels. All energies are in keV.

E_1	E_i	E_2	$i_{\gamma\gamma}$	E_1	E_i	E_2	$i_{\gamma\gamma}$
6753.2	972.0(1)	941.4	56(7)	3263.0	4462.2(3)	4462.2	29(4)
6711.9	1013.3(2)	1013.3	326(20)	3128.4	4596.8(3)	*4596.8	95(10)
		982.7	588(19)			*4566.2	17(7)
6352.5	1372.7(2)	1372.7	9(4)	3034.0	4691.2(2)	4691.2	4263(93)
		1342.1	73(7)			4660.6	2171(50)
6106.2	1619.0(2)	1588.4	29(5)			*1099.8	174(12)
6102.2	1623.0(2)	1623.0	2135(50)	2985.2	4740.0(3)	*1443.6	26(6)
		1592.4	190(11)	2960.6	4764.6(3)	4764.6	765(40)
5586.5	2138.7(3)	2138.7	419(17)			4734.0	5226(117)
		2108.1	530(13)			3391.6	1628(142)
		1125.1	67(6)			2625.7	998(60)
5523.9	2201.3(1)	2170.7	46(5)			*2108.5	467(28)
5238.2	2487.0(10)	2487.0	52(7)			*1173.1	175(11)
		864.1	134(13)	2881.5	4843.7(8)	*4813.1	18(10)
5069.0	2656.2(2)	2656.2	36(7)	2821.7	4903.5(2)	4903.5	2801(60)
		2625.6	12(4)			3889.9	193(18)
		1642.6	60(5)	2791.8	4933.4(4)	4902.8	17(4)
4737.4	2987.8(3)	2987.8	165(17)	2729.1	4996.1(6)	4996.1	19(7)
		1364.9	201(21)			3623.1	541(81)
4620.5	3104.7(14)	*965.8	77(11)	2709.6	5015.6(1)	4985.0	104(7)
		*832.9	183(12)			4002.0	71(12)
4428.9	3296.3(1)	3265.7	198(11)			*3392.7	181(18)
		1673.4	115(13)			*2876.7	105(16)
		1157.4	41(7)	2590.2	5135.0(2)	5135.0	2907(60)
		640.2	11(3)			5104.4	374(16)
4378.1	3347.1(3)	3347.1	356(30)	2558.0	5167.2(5)	*5136.6	14(4)
		3316.5	23(5)	2548.3	5176.9(3)	5176.9	49(10)
4260.1	3465.1(2)	3465.1	5685(113)	2391.3	5333.9(6)	*3711.0	22(9)
		2451.5	317(24)	2379.7	5345.5(2)	*5345.5	13(4)
		1193.3	285(12)			*5314.9	12(5)
4133.9	3591.3(2)	3591.3	3488(83)			*4331.9	37(10)
		3560.7	686(39)			*3722.6	45(11)
		2577.7	1028(57)	2347.0	5378.2(3)	5378.2	79(7)
		1968.4	55(11)			3755.3	25(9)
		*1319.5	234(11)	2282.8	5442.4(4)	5442.4	26(4)
4054.4	3670.8(3)	*3670.8	23(7)			5411.8	1978(43)
		3640.2	49(7)			*4428.8	268(15)
4015.6	3709.6(2)	3709.6	353(27)			4069.4	726(117)
		3679.0	215(13)			3819.5	51(12)
		*2086.7	33(9)			3303.5	887(54)
3849.1	3876.1(8)	3876.1	1966(53)	2128.8	5596.4(0)	*5565.8	10(4)
		2503.1	440(92)			*4582.8	30(6)
		2253.2	226(23)			*2300.0	91(10)
		*1737.2	44(10)	1984.2	5741.0(5)	*5741.0	6(4)
3824.3	3900.9(5)	3900.9	224(17)			5710.4	499(16)
		2887.3	117(15)			*4118.1	36(9)
		*2278.0	43(11)	1965.4	5759.8(11)	*5759.8	23(4)
		*1629.1	48(6)			*3620.9	36(9)
3789.4	3935.8(2)	3935.8	264(20)	1927.2	5798.0(0)	5798.0	102(7)
		3905.2	168(11)			5767.4	330(13)
		2922.2	138(28)			4425.0	1238(116)
		*2312.9	31(10)			*4175.1	52(11)

Table 1. (cont.)

E_1	E_i	E_2	$i_{\gamma\gamma}$	E_1	E_i	E_2	$i_{\gamma\gamma}$
		*3659.1	45(10)	1101.8	6623.4(1)	6623.4	115(10)
1917.8	5807.4(4)	*5807.4	9(4)			6592.8	146(8)
1864.1	5861.1(1)	5861.1	112(10)			*5609.8	16(4)
1720.2	6005.0(6)	*4382.1	23(10)	1073.5	6651.7(1)	6621.1	252(10)
1705.4	6019.8(1)	6019.8	151(14)			*4512.8	82(11)
		5989.2	18(4)	967.9	6757.3(1)	6726.7	90(8)
		5006.2	37(4)	891.8	6833.4(1)	*6802.8	21(4)
		4396.9	53(13)			*5460.4	87(19)
		*3880.9	29(9)			*5210.5	24(6)
1526.8	6198.4(3)	6198.4	610(27)	870.3	6854.9(1)	*6824.3	57(7)
		6167.8	9(4)	868.2	6857.0(3)	*3869.5	13(5)
		4575.5	244(19)	831.5	6893.7(3)	6893.7	26(4)
		4059.5	141(15)			*6863.1	180(8)
		3926.6	25(6)			5880.1	10(3)
		*2733.1	197(19)			*5270.8	66(10)
1482.8	6242.4(1)	*4869.4	185(48)			4754.8	394(22)
		*4103.5	19(8)			*4237.6	47(6)
1408.4	6316.8(2)	6316.8	1904(33)			*3906.2	22(6)
		*6286.2	20(4)			*3597.3	97(8)
		5303.2	290(12)	548.0	7177.2(2)	7177.2	122(10)
1405.2	6320.0(10)	6320.0	16(4)			6163.6	11(3)
		4048.2	39(5)			5804.2	196(23)
		3023.6	109(7)	454.8	7270.4(1)	7270.4	46(7)
1394.2	6331.0(4)	*5317.4	15(5)			7239.8	82(10)
1283.5	6441.7(1)	6441.7	590(27)			5131.5	58(7)
		5428.1	69(6)			*4998.6	49(4)
		4169.9	108(8)			4614.3	28(3)
1231.7	6493.5(3)	*6462.9	9(2)				

1. The lower estimation of $i_{\gamma\gamma}$ for cascades with $E_1 < 520$ keV or $E_2 < 520$ keV.
2. Only statistical uncertainty of determination of energy and intensity.
3. * The transition is placed into decay scheme of the level E_i for the first time.

 TABLE 2. A list of absolute intensities (per 10^5 decays), $i_{\gamma\gamma}$, of measured two-step cascades and energies, E_1 and E_2 , of the cascade transitions. E_i are energies of the intermediate levels. All energies are in keV.

E_1	E_i	E_2	$i_{\gamma\gamma}$	E_1	E_i	E_2	$i_{\gamma\gamma}$
4694.9	3030.3(3)	2999.7	18(10)	4244.3	3480.9(7)	2107.9	493(99)
		891.4	44(8)			1342.0	53(10)
4485.2	3240.0(5)	3209.4	21(7)	4186.6	3538.6(9)	1915.7	27(9)
		1101.1	30(6)			882.5	12(7)
4432.7	3292.5(5)	3292.5	9(4)	4126.4	3598.8(7)	3598.8	56(10)
		1153.6	12(5)			1327.0	34(6)
4424.5	3300.7(6)	644.6	10(3)	3975.3	3749.9(10)	3749.9	16(7)
4281.6	3443.6(3)	1820.7	19(10)			453.5	34(5)
		1304.7	126(15)	3820.4	3904.8(3)	608.4	17(4)
4251.0	3474.2(4)	1335.3	25(7)	3544.9	4180.3(9)	4180.3	13(7)
		1202.4	32(6)	3330.7	4394.5(9)	1407.0	31(8)

Table 2. (cont.)

E_1	E_i	E_2	$i_{\gamma\gamma}$	E_1	E_i	E_2	$i_{\gamma\gamma}$
3301.8	4423.4(6)	1098.1	17(7)	1671.9	6053.3(2)	3914.4	59(10)
		4423.4	13(4)	1623.5	6101.7(5)	6071.1	15(4)
		2151.6	20(7)			3114.2	37(8)
		1318.2	178(28)	1589.6	6135.6(3)	2839.2	26(6)
3146.6	4578.6(2)	831.9	67(8)	1475.0	6250.2(2)	2953.8	41(7)
		1591.1	42(9)	1430.0	6295.2(5)	2998.8	15(6)
		1282.2	42(5)	1363.8	6361.4(2)	4222.5	75(12)
3111.0	4614.2(8)	2475.3	21(7)	1343.3	6381.9(1)	4759.0	15(8)
		1317.8	98(6)			4110.1	19(6)
3075.4	4649.8(3)	4619.2	31(7)			3394.4	154(17)
		1662.3	9(4)			3276.7	140(27)
		4691.2	31(11)	1192.6	6532.6(1)	3236.2	116(10)
2954.9	4770.3(3)	4770.3	92(17)	1174.5	6550.7(1)	3563.2	25(8)
2578.4	5146.8(3)	5116.2	18(5)			3085.4	23(7)
2518.2	5207.0(5)	2935.2	29(10)	1137.1	6588.1(3)	4449.2	28(6)
2450.8	5274.4(6)	5243.8	10(4)	1129.9	6595.3(6)	3298.9	16(8)
2443.3	5281.9(4)	3143.0	28(8)	1125.0	6600.2(1)	3303.8	70(8)
2426.1	5299.1(4)	3027.3	53(11)	1120.7	6604.5(2)	5590.9	27(4)
2422.8	5302.4(3)	3030.6	56(12)	1064.6	6660.6(2)	6630.0	14(4)
2419.9	5305.3(7)	5305.3	6(4)	1024.2	6701.0(5)	3404.6	17(8)
2309.9	5415.3(4)	5415.3	9(4)	983.2	6742.0(4)	6742.0	6(4)
2271.8	5453.4(2)	5453.4	165(10)			3754.5	120(17)
		3830.5	59(12)	941.6	6783.6(3)	4644.7	25(7)
2222.0	5503.2(5)	3880.3	30(10)	910.9	6814.3(4)	4675.4	19(6)
2172.0	5553.2(3)	3281.4	30(7)	878.9	6846.3(7)	4190.2	10(5)
		2565.7	36(9)	815.3	6909.9(4)	3922.4	10(5)
2140.2	5585.0(4)	4571.4	22(6)	787.2	6938.0(3)	6938.0	125(10)
2137.1	5588.1(3)	2482.9	196(42)			3472.7	33(8)
2109.8	5615.4(1)	2627.9	495(32)	588.3	7136.9(1)	7136.9	59(7)
2081.5	5643.7(7)	4630.1	20(9)			6123.3	12(3)
2036.4	5688.8(5)	5688.8	6(4)	381.0	7344.2(1)	7344.2	66(7)
2011.1	5714.1(5)	3575.2	22(7)			5721.3	34(6)
1938.4	5786.8(6)	4163.9	28(10)			5205.3	27(5)
1935.1	5790.1(6)	4167.2	25(9)	315.7	7409.5(2)	7409.5	49(10)
1780.4	5944.8(2)	2957.3	111(15)			7378.9	17(5)

tions. The latter were determined in the usual manner from the spectra of the secondary transitions coinciding with the primary transitions. The same set of $\gamma-\gamma$ coincidences was used for both the determination of b and construction of the spectra like that shown in Fig. 2. The values of the used i_1 and absolute intensities of all observed cascades with these primary transitions are given in Table 3.

The recent data [7] on the intensities of γ -transitions in thermal neutron radiative capture increase our cascade intensities by approximately 10%. One can assume that the data of Ref. [7] are overestimated by that value; the total intensity of the resolved transitions of cascades to the ground state may not exceed 100%, because this spectrum contains also the continuous distribution corresponding to the unresolved cascades of low intensity. Besides, the two-step cascades to the levels with $E_{ex} \geq 3.7$ MeV must also exist. According to the data of Ref. [7], the total intensity of the primary transitions in Tables 1 and 2 alone exceeds 108%.

About a half of the thermal neutron captures is followed (Table 4) by the cas-

cades to the ground and first excited states of ^{28}Al . Exceptionally favourable background conditions permitted us to extract 102 such cascades with the detection threshold $L_c = 10^{-4}$ events per capture. Total intensity of these cascades listed in Tables 1 and 2 is equivalent to $\approx 95\%$ of the total area of two corresponding spectra. This allowed the determination [8] of the energy dependence of cascade intensity in this nucleus with a small systematic uncertainty.

TABLE 3. Energies E_1 and absolute intensities (% of decays) of the primary transitions following thermal neutron capture in ^{27}Al , used for the normalization of the cascade intensities. $\sum i_{\gamma\gamma}$ is the total intensity (% of decays) of the resolved cascades with the listed primary transitions.

E_1 , keV	i_i	$\sum i_{\gamma\gamma}$
6101.31	2.28	2.33(5)
5238.18	0.27	0.19(2)
4428.33	0.73	0.37(3)
4259.54	6.00	6.29(12)
4133.32	6.42	5.49(10)
2960.01	7.99	9.26(20)
Sum	23.7	23.9(3)

TABLE 4. The sum energy $E_1 + E_2$ of cascades and their absolute intensity $I_{\gamma\gamma}$ (% of decays). E_f and J^π are the energy, spin and parity of the cascade final level.

$E_1 + E_2$, keV	$I_{\gamma\gamma}$	E_f , keV	J^π
7725.18	33(2)	0	3^+
7694.54	15.6(14)	30	2^+
6711.55	3.0(2)	1013	3^+
6353.23	3.3(2)	1373	1^+
6102.26	2.2(9)	1620+1623	$1^+, 2^+$
5586.26	3.5(3)	2139	2^+
5453.41	1.3(1)	2272	4^+
5069.09	0.73(4)	2655	4^+
4737.65	[1.2]*	2988	$(1,3)^+$
4620.00	[0.5]*	3105	$(1,3)^+$
4428.79	1.0(1)	3296	3^+
4259.89	[0.5]*	3591	3^-
4133.73	0.6(1)		
Sum	97.9(3)**		

* Estimation from the area ratios of the nearest peaks with a correction by the mean over the spectrum efficiency of registration of cascades.

** Intensity of the primary transitions to the ground and first excited states $I_1 = 31.5\%$ was added.

3. Analysis of experimental data

Qualitative analysis of experimental data on the two-step cascades for all 50 studied nuclei shows that it is necessary to take into account the influence of nuclear vibrations with a phonon energy of about several hundreds keV on nuclear properties for the further development of models of nuclei. This follows from the observation (and strong influence on the observed cascade intensities) of vibrational “bands” built on excited states. This very qualitative conclusion was done in Ref. [9] on the grounds of analysis of the excitation spectra of intermediate levels of the most intense cascades. This is a development of the method tested earlier in Ref. [10].

The authors of Ref. [9] suggested a search for the regularity in the excitation spectra of the intermediate levels of the most intense cascades by means of the auto-correlation analysis of cascade intensities. Only the cascades whose intensities exceed a given selection threshold are involved in analysis. Following this procedure, absolute intensities of the cascades (Tables 1 and 2) proceeding via the same intermediate level are summed. Then the summed intensities are “smoothed” by means of the Gaussian function $f(E) = \sum_E i_{\gamma\gamma} \times \exp(-0.5(\Delta E/\sigma)^2)$ with, for example, parameter $\sigma = 25$ keV. The sum of these smoothed functionals gives the resulting spectrum $F(E)$. Generally, energy dependence of the cascade intensities is to be taken into account. Then the resulting spectrum $F(E)$ is divided by the analogous functional formed with the parameter $\sigma = 250$ keV. This operation cannot result in false equidistant periods.

The values of the auto-correlation function

$$A(T) = \sum F(E) * F(E + T) * F(E + 2T) \quad (1)$$

for different selection of thresholds of intense cascades are shown in Fig. 3 and the distribution $F(E)$ is shown in Fig. 4. The auto-correlation function $A(T)$ has the maximum if the distribution $F(E)$ has at least three equidistant peaks (uncertainty in the determination of the equidistant period for three and more peaks approximately equals σ). The problems of revealing such regularities were analysed earlier [10]. It was shown that even real equidistant “bands” in the spectra of nuclear excitations are not found in some cases, and besides of the corresponding maximum, function $A(T)$ has extrema.

The most probable equidistant period for a specific nucleus in this situation can be found from a comparison of the $A(T)$ values for different selections of the thresholds L_c with the probable equidistant periods in different nuclei. Existence of the equidistant period can be unambiguously proved in the experiments on the study of the two-step cascades in different resonances of the same nucleus, and comparing of results of analysis of Ref. [9] for each of them.

Figure 3 shows the $A(T)$ values for $L_c = 10$ and 50 events per 10^4 decays of the compound state. As it is seen from this figure, the most probable value of the equidistant period T of ^{28}Al is equal to or divisible by 560 keV. This is confirmed by Fig. 4 where together with the dependence of the smoothed intensity of

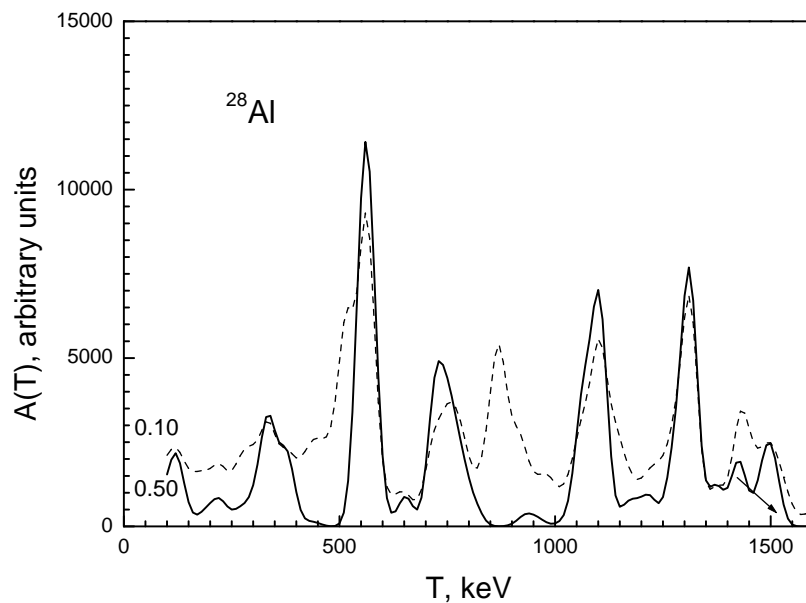


Fig. 3. The value of the functional $A(T)$ for two selection thresholds of the most intense cascades.

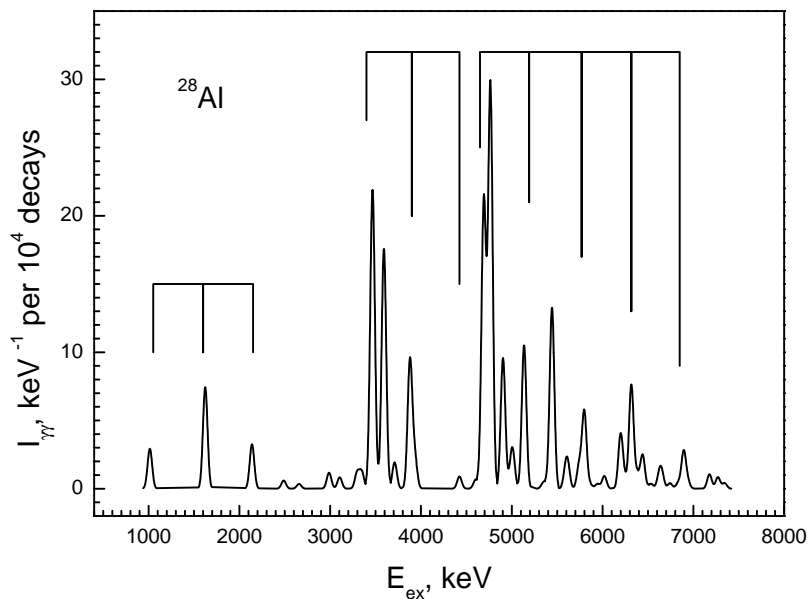


Fig. 4. Dependence of the “smoothed” intensities of cascades listed in Tables 1 and 2 on the excitation energy. Possible “bands” of practically harmonic excitations of the nucleus are marked. The parameter $\sigma = 25$ keV was used.

cascades from Tables 1 and 2 on the energy of their intermediate levels are also shown probable equidistant “bands ” of intermediate levels. In the framework of the conventional nuclear models, the observed harmonicity can be related only with vibrational excitations of the nucleus. Integer value of their spins determine their probable belonging to the system of boson excitations.

Unfortunately, the confidence level of observation of harmonic vibrations in a nucleus with the period of several hundreds keV (probably – “vibrational bands” built on the excited state with complicated structure) is limited by the size of the statistical ensemble (cascades are studied only in 50 nuclei and only in reactions induced by thermal neutrons).

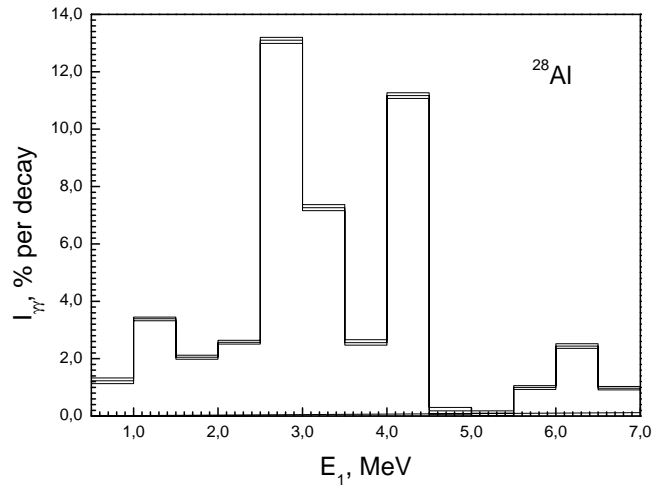


Fig. 5. Experimental distribution of the total intensity (summed in the 0.5 MeV energy bins) of the two-step cascades as a function of the primary transition energy. Only statistical errors are shown.

The dependence of cascade intensity (summed over 0.5 MeV energy bins) on the energy of their primary transitions $E_1 = B_n - E_{ex}$, obtained in accordance with Ref. [8], is presented in Fig. 5. It is seen from the figure that the structure of the excited states of ^{28}Al at $E_{ex} = 4 - 5$ MeV strongly differs from the structure of lower-lying levels.

4. Conclusion

A comprehensive analysis of both spectroscopic and integral information on the two-step cascades proceeding between the compound state (neutron resonance) and a group of low-lying levels of ^{28}Al allowed us to derive its reliable decay scheme in the excitation region that was not studied previously. We confirmed a considerable

influence of vibrational states on the nuclear structure and the presence of cascade γ -decay in a wide range of excitation energy.

Acknowledgements

This work was supported by GACR under contract *N*^o. 202/97/K038 and by RFBR Grant *N*^o. 99-02-17863.

References

- [1] J. Honzátko et al., Nucl. Instr. and Meth. A **376** (1996) 434.
- [2] S. T. Boneva, E. V. Vasilieva, Yu. P. Popov, A. M. Sukhovej and V. A. Khitrov, Sov. J. Part. Nucl. **22**(2) (1991) 232.
- [3] A. M. Sukhovej, V. A. Khitrov, Instr. Exp. Tech. **27** (1984) 1071.
- [4] E. P. Grigoriev, V. A. Khitrov, A. M. Sukhovej and E. V. Vasilieva, Fizika B (Zagreb) **9** (2000) 147; V. A. Bondarenko, J. Honzátko, V. A. Khitrov, A. M. Sukhovej, I. Tomandl, Fizika B (Zagreb) **11** (2002) 201.
- [5] Yu. P. Popov, A. M. Sukhovej, V. A. Khitrov and Yu. S. Yazvitsky, Izv. AN SSSR, Ser. Fiz. **48** (1984) 1830.
- [6] M. A. Lone, R. A. Leavitt and D. A. Harrison, Nuclear Data Tables. **26**(6) (1981) 511.
- [7] R. C. Reedy and S. C. Frankle, Atom. Data and Nuc. Data Tab. **80**(1) (2002) 1.
- [8] S. T. Boneva, V. A. Khitrov, A. M. Sukhovej, Nucl. Phys. A **589** (1995) 293.
- [9] A. M. Sukhovej and V. A. Khitrov, Bull. Russian Academy of Sciences, Physics **61**(11) (1997) 1611.
- [10] E. V. Vasilieva et al., Bull. Russian Academy of Sciences, Physics **57** (1993) 1582.

DVOJNE KASKADE NAKON UHVATA TERMIČKIH NEUTRONA U ²⁷Al

Proučavali smo kaskade dvaju uzastopnih γ -prijelaza koji slijede uhvat termičkih neutrona u ²⁷Al. Na osnovi u mjerenju sakupljenih $\gamma - \gamma$ sudesa, odredili smo 13 raspodjela intenziteta dvojnih kaskada koje završavaju na niskim stanjima ²⁸Al. Iz tih smo spektara izveli energije γ -prijelaza i intenzitete 249 kaskada koje prolaze preko 123 međustanja. Odredili smo također energijsku ovisnost intenziteta zbrojenih preko intervala širine 0.5 MeV za kaskade prema dvama nižim stanjima.